CrossMark

ORIGINAL ARTICLE

Elastic moduli of simple mass spring models

Maciej Kot · Hiroshi Nagahashi · Piotr Szymczak

Abstract Mass spring models (MSMs) are a popular choice for representation of soft bodies in computer graphics and virtual reality applications. In this paper, we investigate physical properties of the simplest MSMs composed of mass points and linear springs. The nodes are either placed on a cubic lattice or positioned randomly within the system. We calculate the elastic moduli for such models and relate the results to other studies. We show that there is a well-defined relationship between the geometric characteristics of the MSM systems and physical properties of the modeled materials. It is also demonstrated that these models exhibit a proper convergence to a unique solution upon mesh refinement and thus can represent elastic materials with a high precision.

Keywords Mass spring model · Soft body deformation · Physically based modeling

1 Introduction

Mass spring models (MSMs, or lattice spring models, LSMs) provide a simple and easy to implement method for the simulation of the behavior of deformable objects. Using MSM is a popular approach for modeling soft bodies in virtual reality (VR) applications as well as computer graphics (CG) [13,14]. In particular, MSMs may be useful for simulating

M. Kot (✉) · H. Nagahashi
Imaging Science and Engineering Laboratory,
Tokyo Institute of Technology, Tokyo, Japan
e-mail: eustachy@gmail.com

P. Szymczak
Faculty of Physics, Institute of Theoretical Physics,
University of Warsaw, Warsaw, Poland

fracture and crack propagation [9]. MSMs are believed to be fast, but not as accurate as the alternatives such as FEM (*finite element method*). Physical correctness greatly helps to improve plausibility of any CG application, and for some of them is absolutely essential (i.e., VR environment involving both interaction and feedback). For the MSM to be physically correct, a relationship needs to be established between spring constants and the real physical properties of modeled materials.

Although MSMs have been carefully investigated by many CG researchers, some of the results and ideas from the classical theory of elasticity did not seem to percolate into CG community. A good example is provided by the problem of calculating the Poisson's ratio of the mass spring model. A well-established result of the continuum mechanics is that the Poisson's ratio of a homogeneous and isotropic material is identically 1/4 (or 1/3 for a 2D system), if the constituents of this material interact with the central forces dependent upon distance alone [7,12]. Unfortunately, many of the studies of mass spring models do not seem to recognize this fact: either trying to estimate the Poisson's ratio of their models (and finding invariably that it is close to 1/4 or 1/3) [1,3,11] or even trying to impose a different value of the Poisson's ratio, a task doomed to failure [17,19]. This has lead to the conviction in CG community that MSMs cannot represent elastic materials accurately and that they do not converge to the exact solution of elasticity equations when their resolution is increased [14].

The purpose of this work is to clarify what can and what cannot be achieved with simple mass spring models, when trying to represent a homogeneous isotropic elastic material characterized by specific elastic moduli using models of arbitrary resolutions. We present both theoretical predictions of elastic parameters as well as their verifications in several test cases. First we discuss lattice-based MSMs, the charac-

teristics of which have been extensively studied in physics and mechanical engineering communities. Next we focus on a more general case and study the properties of disordered MSMs, where the nodes are generated probabilistically. We illustrate our approach with an example of random MSM with particularly simple node placement rules; however, our theoretical results are very general and can be used to assess the elastic properties of any MSM.

It needs to be stressed that this work investigates only the static properties of MSMs. We do not address here the question of how these systems evolve over time or what are the most efficient numerical schemes to track their dynamics; neither we consider the damping characteristics of the springs. Hence, we do not present animations and do not evaluate the efficiency of MSMs in the context of creating an animation (although it is expected to be good [10]). We would like to emphasize that a correct mapping of elastic properties between a physical object and a model is a prerequisite for any physically correct simulation, be it quasi-static or dynamic, and the establishment of this base is the main goal of this work. Efficient ways of simulating dynamics of these systems can be found, e.g., in [10,16].

As in every expanding field, the literature on the topic covers by now a large number of publications. It would be impossible to list all the relevant articles, we therefore direct the reader to the review article by Ostoja-Starzewski [15], which presents physically oriented approach to the different types of MSMs as well as approaches of estimating their physical properties. Another publication discussing MSM approaches, particularly in the context of CG, is the paper by San-Vicente et al. [17]. An extensive survey of deformable modeling in computer graphics can be found, e.g., in Nealen and Müller et al. [14], whereas Meier et al. [13] summarize approaches focused on surgery simulation applications, which offer a more detailed analysis of MSMs.

2 Linear elasticity

In this section, we introduce some basic linear elasticity results that can be found, e.g., in [12] and [8].

A basic assumption of linear elasticity theory is that stress in an elastic body is a linear function of the strain:

$$\sigma_{ij} = C_{ijkl}\epsilon_{kl}, \qquad (1)$$

where $\hat{\sigma}$ denotes stress tensor, $\hat{\epsilon}$ - deformation (strain) tensor and $\hat{C}$ the elastic moduli tensor. Both $\hat{\sigma}$ and $\hat{\epsilon}$ are symmetrical from which it follows that in three dimensions $\hat{C}$ has 21 independent coefficients. This number is reduced to 2 if we assume that the material is isotropic. In such case, $\hat{C}$ can be expressed as

$$C_{ijkl} = \lambda\delta_{ij}\delta_{kl} + \mu(\delta_{ik}\delta_{jl} + \delta_{il}\delta_{jk}) \qquad (2)$$

where δ_{ij} is the Kronecker delta. The relation (1) now becomes

$$\sigma_{ij} = \lambda\delta_{ij}\delta_{kl}\epsilon_{kl} + 2\mu\epsilon_{ij}, \qquad (3)$$

or equivalently:

$$\sigma_{ij} = K\delta_{ij}\epsilon_{kk} + 2\mu(\epsilon_{ij} - Tr(I)^{-1}\delta_{ij}\epsilon_{kk}), \qquad (4)$$

where λ and μ are Lamé parameters, I is an identity matrix and K is a bulk modulus obeying $K = \lambda + \frac{2}{3}\mu$ in 3D or $K_{2D} = \lambda + \mu$ in 2D. Einstein summation notation is used here (i.e., the appearance of a repeated index in a term implies summation over it, e.g., $\epsilon_{kk} = \sum_{k=1}^{d}\epsilon_{kk}$, where d is dimensionality of the space).

Elastic energy F of a deformed body is given by

$$F = \frac{1}{2}\sigma_{ij}\epsilon_{ij} = \frac{1}{2}\lambda(\epsilon_{ii})^2 + \mu\epsilon_{jk}^2, \qquad (5)$$

whereas the equation of motion reads

$$\rho\frac{\partial^2\bar{u}}{\partial t^2} = \lambda\nabla(\nabla\cdot\bar{u}) + \mu(\nabla^2\bar{u} + \nabla(\nabla\cdot\bar{u})), \qquad (6)$$

where $\bar{u}$ is a displacement and ρ mass density.

The relative change of the volume of a body can be expressed by strain as:

$$\frac{V+\Delta V}{V} = (1+\epsilon_{11})(1+\epsilon_{22})(1+\epsilon_{33}) \approx 1+\epsilon_{11}+\epsilon_{22}+\epsilon_{33}, \qquad (7)$$

therefore in accordance with Eq. (4), K gives the resistance to compression. It can also be defined as:

$$K = -V\frac{dp}{dV}, \qquad (8)$$

where V is the volume of a solid body, and p pressure acting on its surface.

Beside λ, μ and K, two other elastic parameters are often defined—the Young's modulus E and the Poisson's ratio ν. The Young's modulus is the ratio of stress to strain measured along the same axis under an uniaxial stress condition, whereas the Poisson's ratio is the ratio of transverse to axial strain, i.e., $E = \sigma_{xx}/\epsilon_{xx}$ and $\nu = -\epsilon_{yy}/\epsilon_{xx}$, in an experiment where all components of the stress tensor are zero except σ_{xx}. The above parameters can be expressed in terms of λ and μ:

$$E = \frac{\mu(3\lambda + 2\mu)}{\lambda + \mu} \quad \nu = \frac{\lambda}{2(\lambda + \mu)}, \qquad (9)$$

or

$$E_{2D} = \frac{4\mu(\lambda + \mu)}{\lambda + 2\mu} \quad \nu_{2D} = \frac{\lambda}{\lambda + 2\mu}. \tag{10}$$

Any two of the above-discussed parameters are sufficient to describe elastic properties of an isotropic material, thus given any two, any other of the elastic moduli can be calculated.

The assumption that all the internal forces in the material are the central forces [i.e., that they can be represented by the potential $V(r)$, with r—the distance between the particles] leads to 6 additional relations between the components of C_{ijkl} (note B in [12]). Thus in a non-isotropic case $\hat{C}$ will have 15 independent coefficients instead of 21, and for an isotropic material 1 instead of 2. In the latter case $\lambda = \mu$, from which it follows that

$$\nu = 1/4 \quad \nu_{2D} = 1/3. \tag{11}$$

3 Mass spring models

Mass spring models represent an elastic material by means of discretization. It is important to note that in such representations there are two things that are discretized. The first is a mass distribution which in real materials is usually treated as continuous, the second, represented by springs, characterizes the interactions between the material points and thus defines elastic properties of a physical body. Both of these aspects are important and will affect the realistic appearance of simulated objects. If we increase the number of mass points representing an object, the resolution of the model becomes higher resulting in a more faithful representation of the deformations. On the other hand, increasing the number of springs attached to each mass point allows one to represent the local elastic properties of the material in a more accurate way.

We emphasize the distinction between these two aspects because in most popular variants of the mass spring models, the springs connect the neighboring nodes only. In principle, however, one can introduce also the connections between the further nodes. This means that such networks cannot be decomposed into a sum of non-overlapping volumetric primitives, as it is the case in other discretization approaches (e.g., FEM). Some of the systems analyzed in the present study are of this kind.

As already mentioned, independently of the discretization technique, if only radial springs are used, then, in accordance with (11), any isotropic homogeneous structure will have a fixed value of Poisson's ratio. Other values of the Poisson's ratio can be obtained by incorporating non-central forces into the model, e.g., the angular terms, or forces that do not depend on distance alone or by introducing anisotropy [7].

Such extensions are often present in more advanced models [1,11].

3.1 Triangular lattice MSMs (2D)

While this work is focused on volumetric objects and their MSM representations, for completeness we include a brief discussion of the two-dimensional networks. Much attention in computer graphics has been given to two-dimensional MSMs (mostly for the purpose of the cloth representation) and many advanced models have been created. The body of work on the subject is quite extensive, and it is not our intention to review this area. Instead, we focus on the simplest triangular meshes capable of representing isotropic materials.

In one of the pioneering CG works on this topic Van Gelder [19] analyzes 2D spring meshes and tries to find the spring stiffness coefficients that would allow mass spring model to behave like a reference FEM model.

The results seem to be discouraging, with the author stating that "assigning the same stiffness to all springs badly fails to simulate a uniform elastic membrane". It seems, however, that part of the problem here is the attempt to represent materials with arbitrary values of ν, whereas as it was already noted only $\nu = 1/3$ materials can be modeled with radial 2D spring networks. For such materials, the 2D MSM models based on hexagonal lattice and uniform stiffness coefficients were shown to perform reliably [6,11,15]. The use of hexagonal lattice (composed of equilateral triangles) is necessary to retain the isotropy of the system [15]. Another potential problem in [19] is that the calculation of elastic properties is performed for a single triangular element of the network, whereas the elastic response of the system will also depend on the relative placement of such triangles in the periodic cell.

The relation between the spring coefficient k and the Lamé constants for a hexagonal network is given by

$$\lambda = \mu = \frac{3}{4\sqrt{3}}k, \tag{12}$$

from which all the other elastic moduli can be derived (note that there is a typo in this particular expression in [15]).

This model can be easily extended to achieve other values of ν by incorporating angular springs between triangle edges which is known as a Kirkwood model of an isotropic material [15]. Elastic moduli are then given by

$$K_{2D} = \frac{3}{2\sqrt{3}}k \quad \nu_{2D} = \left(1 - \frac{3\beta}{2ka^2}\right)\Big/\left(3 + \frac{3\beta}{2ka^2}\right), \tag{13}$$

where a is a length of an edge of a triangle, k is a spring stiffness coefficient of regular springs and β of angular ones. As observed, $\nu_{2D} \to 1/3$ when $\beta \to 0$.

As mentioned above, the fact that $\nu_{2D} = 1/3$, is a general property of central force models and it usually resurfaces in one form or another in any work that investigates such models, even if its analytical justification is unknown to the authors. For example Delingette [3], while analyzing similar triangular meshes notices that "without the addition of angular springs, MSMs with the right stiffness parameters can at best approximate the behavior of a membrane with $\nu_{2D} = 1/3$.". Lloyd et al. [11] arrive at Eq. (12) and also notice that membranes can be better approximated when $\nu = 1/3$, than for other values of ν, not recognizing, however, that it is not an approximation but an exact result for the model chosen.

3.2 Cubic lattice MSMs

Just as hexagonal lattice MSM in two dimensions, a cubic lattice MSM can be used to represent homogeneous isotropic materials in 3D, if the connections between the nodes and their stiffnesses are chosen in an appropriate way [6].

Unfortunately, there is no work in CG that satisfactory explores the properties of such networks. The most recent publication on this topic is by San Vicente et al. [17]. It runs, however, into similar problems to van Gelder's work discussed above—the authors attempt to impose the values of the Poisson's ratio different from 1/4 (which is an exact result for any 3D radial spring network) and match the behavior of FEM models with MSM. The performance of their model is rather questionable, as even in the test of simple bending, the deformation (and thus also the elastic moduli) seems to depend strongly on the resolution of the MSM, in contrast to the results shown in the present work (*cf.* Sec. 5.3). Comparison of Fig 10. in [17] with Fig. 14 of the present article shows that the cubic MSMs considered here show almost no dependence on the resolution and are thus better suited for the practical applications.

Contrary to what is suggested in [17] an isotropic system can be reliably modeled with 3D cubic lattices, provided the connectives and spring stiffnesses are chosen in an appropriate way. The models of that kind were constructed in [6]. The two simplest variants have 18 and 14 connections per node, respectively. The first model allows nearest-neighbor and next-nearest-neighbor connections (group A and B in Fig. 1), all with the same spring coefficient k. The second model uses A-springs with $k = \kappa$, and C-springs with $k = \frac{3}{8}\kappa$, however it is reported to be less stable.

In both cases, the macroscopic displacement field of the spring network is shown to obey

$$\rho \partial_t^2 \bar{u} = \frac{k}{a}[2\nabla\nabla \cdot \bar{u} + \nabla^2 \bar{u}] + O(\nabla^4 u), \tag{14}$$

where a is the length of an edge of an elemental cube, and $\bar{u}$ the displacement vector.
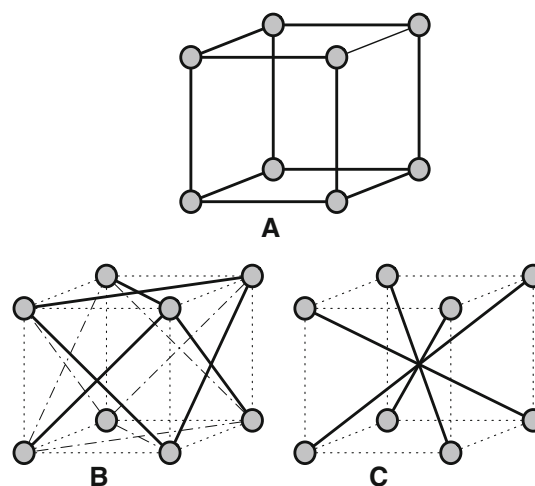
Fig. 1 Elementary cell of a cubic lattice; three types of spring connections. **a** Springs between nearest neighbors, **b** springs along face diagonals and **c** along cube diagonals

From Eq. (6), we can see that both Lamé constants have the same value, equal to k/a. Using Eq. (9) we can write E and ν as a function of k and a:

$$E = \frac{\mu(3\lambda + 2\mu)}{\lambda + \mu} = 2.5\frac{k}{a} \quad \nu = \frac{\lambda}{2(\lambda + \mu)} = 1/4. \tag{15}$$

Note that this MSM is constructed as a *superposition* of cubical elements. For each "element", the corresponding mass is distributed equally into its corners. When two elements are placed beside each other, their corners (masses) coincide, and the effective mass at these points increases. Analogously spring coefficients increase as well. Therefore, to get a correct representation of boundaries, masses placed on a border of an object have to be smaller and springs weaker with comparison to those inside the object. A single cubical element with mass m has $\frac{1}{8}m$ at each corner, its A-springs have $k = 0.25\kappa$ and B-springs $k = 0.5\kappa$. Such construction allows to represent boundaries in a convenient way, however, it has some drawbacks, which we will discuss in detail in Sect. 5.3.

Another work that tackled the problem of cubic MSMs for CG applications is Baudet et al. [1]. They present an extended MSM capable of representing materials with ν other than 1/4. However, in their numerical analysis they treat Young's modulus, Poisson's ratio, shear modulus and bulk modulus as four independent quantities, not recognizing that only two of them are independent, and in case of radial springs—only one. Hence, by imposing four arbitrary values for these quantities, they run into a risk of constructing a self-contradictory problem, which cannot be resolved, no matter what values of spring coefficients are used. Despite that, they arrive at $\nu = 1/4$ solution, but discard it as not versatile and unsatisfying. Instead they introduce additional "orthogonal correction

force" to the model, which effectively allows to achieve other values of ν. Such *extended MSM* performs entirely satisfactory in compression and shearing tests for $0.1 < \nu < 0.5$, with errors being minimal for $\nu = 0.25$, however the results of the bending test are again strongly dependent on the resolution, similarly as in [17].

3.3 Disordered MSMs

Cubic MSMs are simple and their properties are well defined as elucidated in the previous section, however in some situations it is beneficial to relax the constraint of regular placement of mass points and consider disordered placement of the nodes.

Such models have been analyzed by Lloyd et al. [11], who obtain an approximate solution for the values of spring parameters by a minimization procedure which tries to match the behavior of FEM elements with tetrahedral MSM elements. The core of the discretization procedure used by these authors is to decompose the object into a set of primitives (tetrahedra) which do not overlap except along the faces. Such FEM-like representations prove to be convenient, because the total elastic response of the system can be expressed as the sum over primitives, the properties of which can be calculated in a relatively simple manner (cubic lattice MSMs belong to this group as well). However, the issue with tetrahedral meshes is that 3D space cannot be filled with regular tetrahedra. A single tetrahedron is also not an isotropic structure, therefore, it is problematic to define elastic moduli for a tetrahedron. Quantities such as energy density required for a uniform compression may still be estimated (from which the bulk modulus can be derived), because they do not depend on the isotropy of the system. Many CG works succeed in doing that (e.g., [1,11,17]). The complete behavior of an MSM cannot, however, be derived from the behavior of a single tetrahedron without considering the relative placement and properties of other tetrahedra in the network (and these properties will vary, because not all the tetrahedra can be regular).

In contrast, in this work we abandon the FEM-like approach of constructing objects out of volumetric primitives. Instead, we propose a node-centered approach in which the mass points are the basic building blocks, to which any number of springs can be attached representing the channels along which the momentum is transported throughout the system. In this way, we gain the flexibility of adjusting the network connectivity, which is a powerful tool for improving local behavior of the network.

To stay as general as possible, we will perform numerical experiments on MSMs constructed with a very few assumptions about the node placement as well as simple connection rules. First, we generate the positions of the nodes using *random sequential addition algorithm* [18], which simply means that we iteratively pick random positions within the
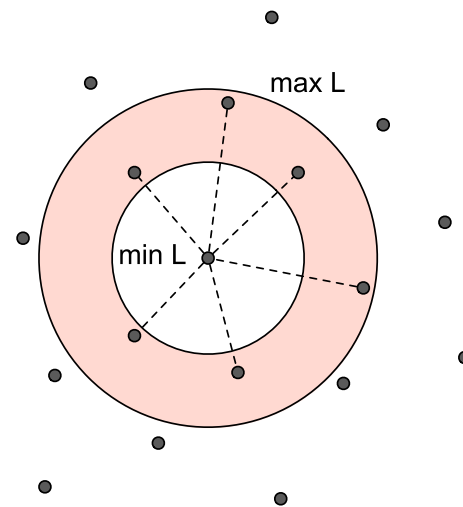
Fig. 2 Random point distribution. Example of spring connections for a chosen node (in 2D for better readability; real models are three dimensional). Minimal allowed distance between two points equals *minL*. Maximal range of spring connection—*maxL*

sample and check whether a newly created point is sufficiently separated from the neighboring nodes. If not, the point is discarded and a new position is sampled. The minimal allowed distance between the nodes is given by *minL* parameter (Fig. 2). The procedure runs until it fills the volume with a desired number N of mass points (which may not be possible, if N is too large for a given volume). Next, all nodes which are less than *maxL* apart get connected by springs.

In practice it is more efficient to generate the random nodes in several stages, in smaller parts of the system. In this work, we have used a spherical 'sampling window' with radius $R_s = 3minL$, which advanced through the volume with $\sqrt{2}R_s$ steps. A sphere was chosen to ensure that the shape of boundaries of the system would not influence the isotropy of the node distribution. The initial sampling volume was slightly larger than the size of the system and the nodes positioned outside of the modeled block were discarded in the final step of the MSM generation process.

Random MSMs tested in this work differ by *minL*, *maxL* and the total number of nodes, N (which sets the resolution for a given volume). However it will prove more convenient to express our results in terms of another set of parameters: mean spring length $\langle L \rangle$, standard deviation of the spring lengths d_L and average number of springs attached to a node $\langle S \rangle = 2S_{tot}/N$, where S_{tot} is the total number of springs in the system. We have analyzed models with $\langle L \rangle$ varying from 0.97 to $1.52\,l$, $\langle S \rangle$ from 8.2 to 29 and standard deviation between 0.1 and $0.33\,l$, where l is a characteristic distance between the mass points, $l = (V/N)^{1/3}$. These values correspond to distributions generated with *minL* between 0.81 and $0.94\,l$ and *maxL* between 1.17 and $1.99\,l$.

Treating cubic lattice model as a "random" model with $l = a$ (where a is a lattice constant), $minL = a$ and

$max L$ in the range between $\sqrt{2}a$ and $\sqrt{3}a$ we can introduce a loose correspondence between cubic lattice MSM and random MSM; as it turns out a similar performance can be achieved with roughly the same number of nodes and springs for both models, especially if we consider large scale deformations.

4 Elastic constants of mass spring models

Homogeneous and isotropic medium can be characterized by two independent elastic constants. We have already established that the Poisson's ratio of all the models based on central forces is equal to 1/4, which applies to disordered networks as well. Thus, we need one more elastic parameter to complete the description.

The simplest quantity to calculate is the bulk modulus K [see Eq. (4) and (8)]. To estimate it, let us imagine uniform compression of our system as a result of which all the lengths of the springs are compressed by the same degree

$$L_i' = L_i(1 + \epsilon), \tag{16}$$

where L_i' is the new, compressed length of the i-th spring and $\epsilon < 0$ in case of compression. The change in the energy density associated with this deformation is then

$$\Delta e = \frac{\sum_i \frac{1}{2} k_i \epsilon^2 L_i^2}{V}, \tag{17}$$

where V denotes the volume of the object. However, from the basic elasticity theory [8] Δe in the uniform compression is given by

$$\Delta e = \frac{9}{2} K \epsilon^2. \tag{18}$$

Thus

$$K = \frac{1}{9V} \sum_i k_i L_i^2 = \frac{1}{9} \frac{n \langle S \rangle}{2} \langle k L^2 \rangle, \tag{19}$$

where k_i and L_i denote spring coefficient and natural length of i-th spring, $n = N/V$ is the concentration of the nodes, the average $\langle k L^2 \rangle$ is taken over all the springs in the system and $\langle S \rangle$ over all the nodes and denotes the average number of springs connected to a node (one spring connects two nodes, hence the division by two). Once the bulk modulus (and Poisson's ratio) is known, all the other elastic constants can be estimated, e.g., Young's modulus E:

$$E = 3K(1 - 2\nu) = \frac{1}{6V} \sum_i k_i L_i^2, \tag{20}$$

where $\nu = 1/4$ was assumed in the last equality.

As an example, let us calculate the Young's modulus of the first of the two cubic MSMs discussed in Sect. 3.2. The spring constant is then uniform and the mean square length of the spring reads

$$\langle L^2 \rangle = \frac{6 \cdot 1 + 12 \cdot 2}{18} a^2 = \frac{5}{3} a^2 \tag{21}$$

whereas $\langle S \rangle = 18$. This leads to the bulk modulus:

$$K = \frac{5}{3} \frac{k}{a}, \tag{22}$$

which yields $E = 2.5\frac{k}{a}$ if we take $\nu = 0.25$, giving the same result as the one obtained previously. It is easy to show that the same value is obtained in the case of the second model of Sect. 3.2 as well.

The Eqs. (19) and (20) allow one to calculate the elastic constants of a material modeled with any MSM, not limited to a particular node distribution or spring connection rules. However, the more homogeneous and isotropic the model is, the more faithfully it can be described by the two elastic moduli K (or E) and ν. As we recall, such a two-parameter description is possible for isotropic solids only. Moreover, MSMs are based on linear elasticity theory, and are expected to give a plausible elastic response only within its limits, that is for small relative displacements.

5 Tests

In this section, we will compare the theoretical predictions of Eqs. (19) and (20) with the corresponding values measured as a result of a numerical experiment (which we will refer to as *measurements*). The numerical experiments mimic the real experimental setup used to obtain a given elastic modulus, e.g., to obtain the Young's modulus and Poisson's ratio we measure the deformation of the material during uniaxial compression, as reported in detail below.

5.1 Uniaxial compression

To estimate numerically the values of E and ν the following numerical experiment has been performed: a block cutout of an elastic material was compressed by applying static displacement to its opposite ends along x direction, and the resulting deformation was measured both for random and cubic MSMs. The Young's modulus and Poisson's ratio are related to the elastic response of such a system by

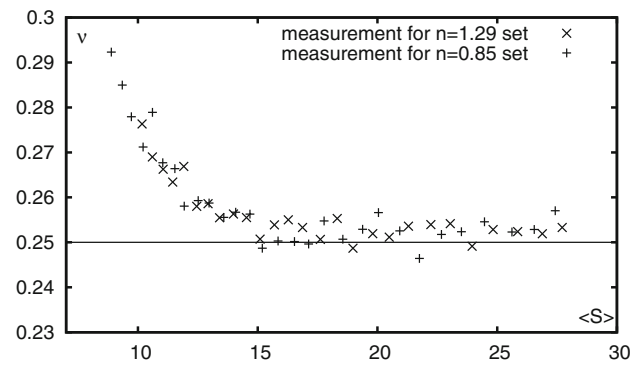$$E = \frac{F/A}{\Delta x / L_x}, \quad \nu = \frac{\Delta y}{\Delta x},$$
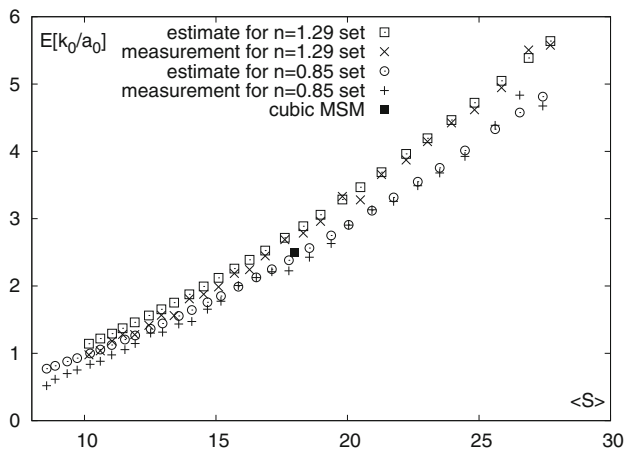
Fig. 3 Young's Modulus for random MSMs with two different $minL$ parameters (varying $maxL$). Set A (*open squares*) with $minL = 0.8a_0$ and $n = 1.29$ nodes per unit volume; set B (*circles*): $minL = 0.9a_0$, $n = 0.85$. The estimates based on Eq. (20) as well as the values measured in the compression test are plotted as a function of the average number of springs per node $\langle S \rangle$. Measurement uncertainty 4 %

Fig. 4 Poisson's ratio for random MSMs from Fig. 3. Theoretical value $\nu = 0.25$. Measurement uncertainty 4 %

Fig. 5 The relative difference between the values of E measured in the compression test and the estimates based on Eq. (20) for random MSM

where F is the reaction force, A the cross-sectional area of the block (in YZ plane), and Δx and Δy are the deformations of the block along x and y directions, respectively. The initial block dimensions were $70a_0 \times 15a_0 \times 15a_0$ (where a_0 is an arbitrary unit of length) and the base spring constant has been set to k_0. The static displacement in x direction was imposed on all the nodes within $1.5maxL$ from the boundary of the block.
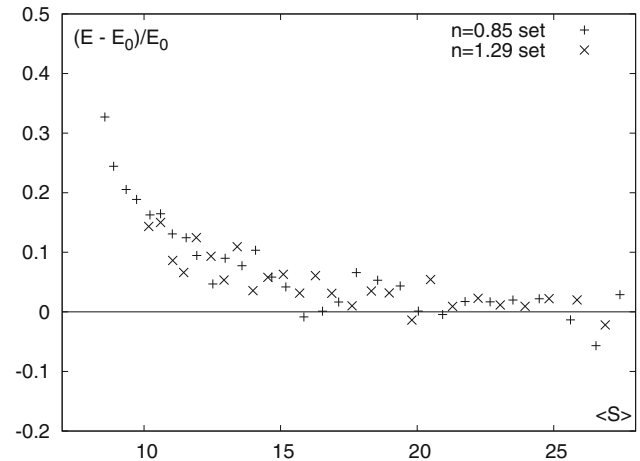
The value of Δy could be measured directly by comparing displacements of extreme points; however, we have not taken any steps to ensure that random MSMs have sufficient connectivity at the boundaries. It happens occasionally that a point with low connectivity behaves like a "floppy tail" introducing additional uncertainty to such measurements. To avoid this problem, we have measured an average expansion Δy of a specific region in the center of the block (by comparing positions of points in deformed and undeformed blocks). The width of this region was set to 80 % of the width of the block. The reaction force was estimated by measuring the momentum flow through the YZ plane in the middle of the system. (By momentum flow across a given plane we understand the sum of the forces in all the springs intersecting the plane projected on the vector normal to that plane).

For the cubic MSM we find that the theoretical estimates based on Eq. (15) differ from the measurement values by no more than 5 % (which can be attributed to measurement errors). Notably, elastic moduli have remained almost constant (within 0.1 %) as the resolution was changed from 8 points per unit length to 1 [5].

The results for random MSM are shown in the Figs. 3 and 4. Two sets of test cases are presented there, with slightly different resolutions ($n = 1.29$ and $n = 0.85$ nodes per unit volume). The values of E and ν are plotted against the average number of springs attached to a node, $\langle S \rangle$. In most of the tests, the value of Poisson's ratio was equal to 1/4 with a good accuracy (within 2 %). Only models with very low $\langle S \rangle$ diverged from this value by more than 5 %. As we can see in Figs. 3 and 5, values of E estimated with the use of Eq. (20) are in a very good agreement with the measured ones. The relative error is smaller than 5 % for almost all the models with $\langle S \rangle$ between 15 and 25. However, for smaller $\langle S \rangle$, discretization errors increase significantly. There is thus a trade-off between the accuracy and computational costs: larger values of $\langle S \rangle$ offer a more accurate representation of the material, which comes, however, at a price of an increased computation time.

As we can see in the experiments, for low connectivity networks, increasing $\langle S \rangle$ increases the accuracy of the estimate in Eq. 19. However, after $\langle S \rangle \approx 15$ is reached, further increase of the number of springs does not improve accuracy. This also means, that for a given number of springs S (spring budget), networks with $\langle S \rangle = 15$ will offer the highest reso-

lution (highest N; most detailed models), while keeping the accuracy at the highest level (provided that the total number of nodes N, is sufficient to form a stable network). One needs to be aware, though, that these estimates are based on the numerical experiments with the random networks constructed according to the procedure presented in Sect. 3.3, and it is conceivable that another way of constructing MSMs might lead to a smaller value of optimal $\langle S \rangle$.

5.2 Point force in an infinite solid

To further validate the model, we have considered a classical problem of linear elasticity, in which a point force is applied to an elastic solid of an infinite extent [2,8]. The strain and stress tensors are then given by:

$$\epsilon_{ij} = \frac{-(1+\nu)}{8\pi E(1-\nu)R^2}\left(\frac{3F_k x_k x_i x_j}{R^3} - \frac{F_k x_k \delta_{ij}}{R} + (1-2\nu)\frac{F_i x_j + F_j x_i}{R}\right), \tag{23}$$

and

$$\sigma_{ij} = \frac{1}{8\pi(1-\nu)R^2}\left(\frac{3F_k x_k x_i x_j}{R^3} + (1-2\nu)\frac{F_i x_j + F_j x_i - \delta_{ij} F_k x_k}{R}\right), \tag{24}$$

where $R = \sqrt{x_i x_i}$ and F is the force (applied at the origin).

In our tests, the solid characterized by $E = 100[\frac{k_0}{a_0}]$ and $\nu = 1/4$ has been modeled as a sphere with radius $5a_0$ represented by a cubic MSM model with $a = 0.25a_0$ and $\langle S \rangle = 18$ as well as three random MSMs with $l \approx 0.25a_0$ and $\langle S \rangle = \{11, 15, 18\}$, which we will refer to as S_{11}, S_{15} and S_{18} models.

A static force $F = 10[k_0 a_0]$ has been applied along y direction to the mass point in the center of the sphere. Stress and strain tensor values were measured at 100 points uniformly distributed along the [1, 1, 1] line from the center of the sphere to its border. Example profiles of strain ϵ_{12} and stress σ_{12} for random MSMs S_{18} and S_{11}, are shown in Figs. 6, 7, 8, and 9. Horizontal axes are scaled in such a way that 0 corresponds to the center of the sphere, and 100—to the border. Smooth red line represents theoretical values. Stress measurements were carried out using Hardy's method [4,20].

Figures 10 and 11 present the mean deviation from theoretical values for the measurements of strain and stress tensors, respectively. We concentrate on the region in the center of the sampling line (points 15–80), to minimize the effect of boundaries as well as the singularity at $r = 0$.

For S_{18} model, all the components of strain and stress tensors are in a good agreement with the theoretical predictions. As could be expected, random MSMs exhibit a somewhat
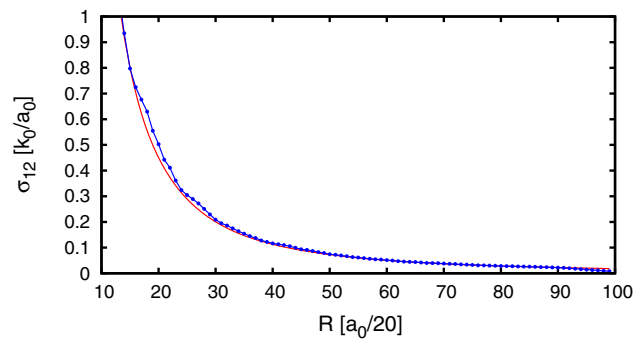

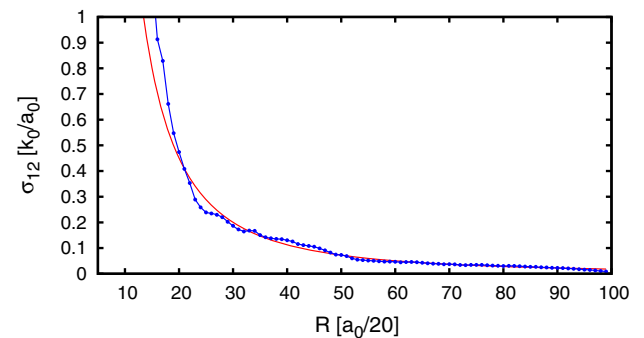**Fig. 6** The stress component σ_{12} for S_{18} random MSM

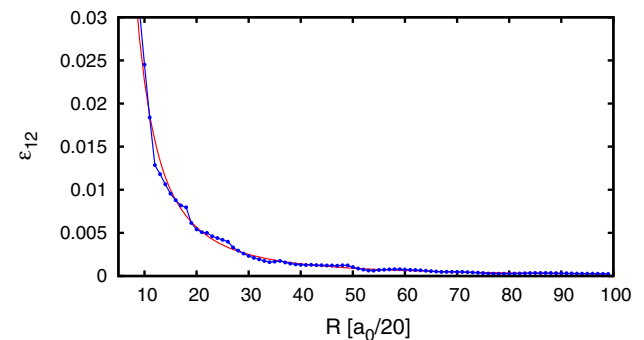**Fig. 7** The stress component σ_{12} for S_{11} random MSM

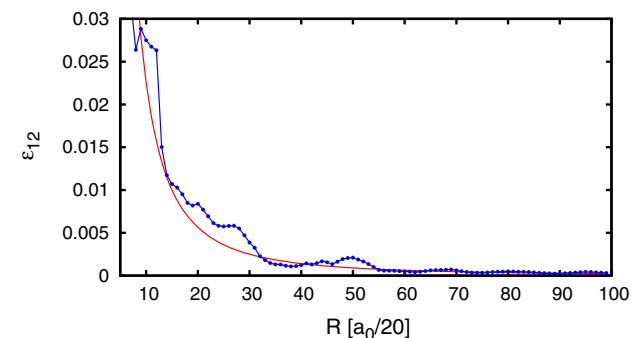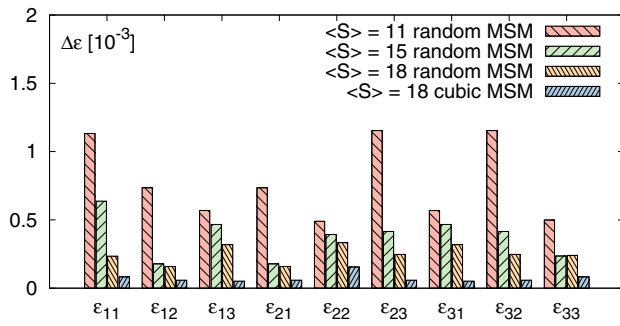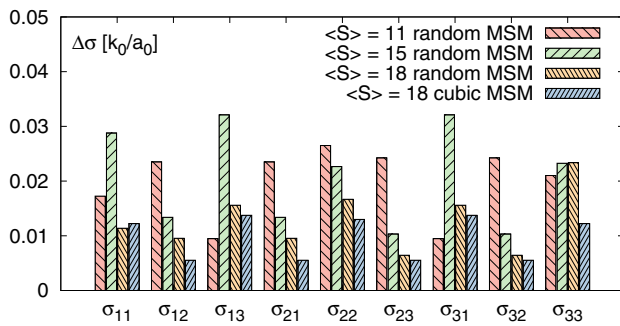**Fig. 8** The strain component ϵ_{12} for S_{18} random MSM

Fig. 9 The strain component ϵ_{12} for S_{11} random MSM

Fig. 10 Mean deviation of the strain components measured in the MSM models from those calculated based on Eq. (23)

Fig. 11 Same as in Fig. 10 but for the stress components

Fig. 12 A segment of a bent beam. *Left* continuous model, *right* lowest possible resolution of cubic MSM

more erratic behavior than cubic lattice MSM; oscillations around theoretical curves are present for all the test cases. For the strain tensor the errors systematically increase as $\langle S \rangle$ is decreased. Stress components, however, do not seem to be affected by the change of $\langle S \rangle$ to the same extend. In the random networks with low $\langle S \rangle$ values, statistical noise plays a significant role, which results in the locally anisotropic and inhomogeneous structures, and corresponding inaccuracies in local node displacements. This, however, does not affect the momentum flow to the same degree, and the network still gives a good elastic response.
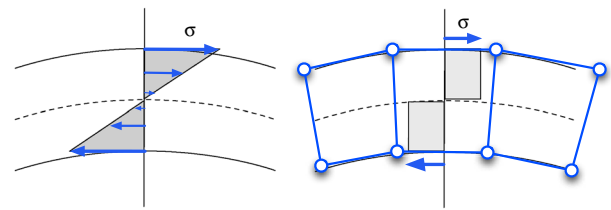
5.3 Deflection test

To verify how our models behave in a typical situation we have performed a deflection test, where a bar of elastic material with dimensions $4a_0 \times 1a_0 \times 1a_0$ bends upon a constant force applied perpendicularly to one of its ends. Besides comparing the numerically measured deflection with the theoretical predictions, one can also directly assess the visual quality of the model.

A deformation of such beam is given by [8]:

$$\Delta y = \frac{F}{E} 2x^2(3L - x), \tag{25}$$

where F is the applied force, E Young's modulus, L length of the beam and x denotes the distance from the fixed end of

the beam. The equation holds for deflections which are small (the radius of the bend) when compared with the thickness of the beam.

As we have mentioned in Sect. 3.3, many popular discretization approaches treat a continuous model as composed of non-overlapping volumetric primitives. This includes cubic lattice described in Sect. 3.2. This experiment exposes a weakness of such approaches. To illustrate the problem let us consider a small segment of a bent beam as shown in the Fig. 12. The upper half of the material is stretched, the lower is compressed and in the middle there is a neutral surface, which does not experience any tension. The total momentum flow through both lower and upper parts is proportional to the force applied at the far end. In continuous model the tension increases linearly with the distance from neutral surface, and the total momentum flow can be calculated as an integral from zero to σ_{max} present near the surface (shaded triangle in Fig. 12). On the other hand, in discretized system, the flow does not change continuously, but is localized on the springs. In case of a beam, which thickness is represented by a single cubical element, this means that the whole momentum flow of the upper and lower parts will be localized on one spring, respectively (shaded square on the Fig. 12). For these two flows to match (continuous and discretized), the strain on the spring has to match the strain in the middle between the neutral surface and the border of a continuous beam. This means that the force applied to low resolution cubic MSM has to be two times larger than corresponding force applied to continuous model, to achieve the same deflection. If the resolution of the discretized model is increased, the stress gradient can be approximated more accurately and the response to a bending force will be closer to the response of continuous model, with the bending force obeying $F_a = F/(1 - 0.5a)$, where a is the length of elementary cube, the thickness of the beam is assumed to be 1 and F is the force applied in the continuous model.

The node-oriented discretization approaches, in which mass of a region of the material is localized in the center of this region, and not distributed into its corners, do not suffer from this artifact. This includes random MSM described in Sect. 3.3. Cubic lattice MSM from Sect. 3.2 can be adapted
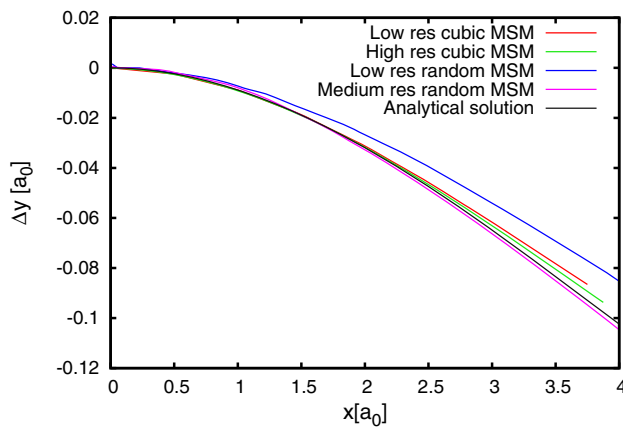
Fig. 13 Deflection test for four different MSMs. Low resolution cubic MSM with the edge of an elemental cube $a = 0.5\,a_0$, number of mass points $N = 32$ and $S = 132$ springs. High resolution cubic MSM, $a = 0.25\,a_0$, $N = 256$, $S = 1632$. Low resolution random MSM, $N = 57$, $S = 258$. Medium resolution random MSM, $N = 161$, $S = 934$. Applied force $F = 0.1[k_0a_0]$, Young's modulus $E = 250\,k_0/a_0$. The origin of the x-axis is placed in the middle of the frozen region

easily as well, by following Eq. 19. The nodes would no longer be placed on the surface of an object, but in the distance $0.5a$ within it (see the leftmost model on the Fig.14). For the example from Fig. 12 it means that springs will be already placed in the middle between neutral surface and the border of the beam and will correctly approximate the momentum flow present in continuous system.

Numerical experiments confirm that the deformation of such models depends only weakly on the resolution of the network. We have tested various resolutions for both cubic and random MSMs. Example profiles of small deflections of four chosen models are presented in Fig. 13, together with theoretical curve. Small differences between low and high resolution cubic MSMs are most likely caused by the change of effective length of the beam caused by discretization (the force is no longer applied precisely at the end of the beam,

but at the point $0.5a$ inside of the beam). We set the origin of x-axis to be in the middle of the frozen region; for random MSM this region extends to $1.1minD$ from the end of the bar, for cubic MSM it is simply the leftmost layer of nodes. Medium resolution random MSM curve should be treated as having 5% uncertainty, and low resolution one as having 10–15 % (based on the changes observed between different runs of the test).

Figure 14 shows results for a bigger force with large deflection. Even though Eq. 25 no longer holds, the deformation of all MSMs remains consistent among different resolutions and MSM types. In all the conducted tests, various resolutions of cubic MSMs behave almost identically. Both medium and low resolution random MSMs behave surprisingly well, exhibiting relatively small deviations from lattice models, which shows that even such unsophisticated method of generating MSM allows one to obtain models with a decent quality.

6 Conclusion and final remarks

In this work we have formulated a methodology for constructing the mass spring models with well-defined physical properties for the use in Computer Graphics. In particular, we emphasized the importance of isotropy of the models and the limitations it places on the geometry of the network. Next, we have discussed the classical result of the theory of elasticity that while any value of the Young's modulus can be obtained by tuning the spring coefficients in the network, the value of the Poisson's ratio is constrained to be 1/4 (in 3D). Finally, we have derived a simple formula, Eq. (20), linking the Young's modulus with the mean value of kL^2 throughout the network, where k and L are the spring stiffness coefficient and its length, respectively. This is a relatively simple and yet general formula which can be applied to virtually any MSM and does not require a complicated analysis of the model.
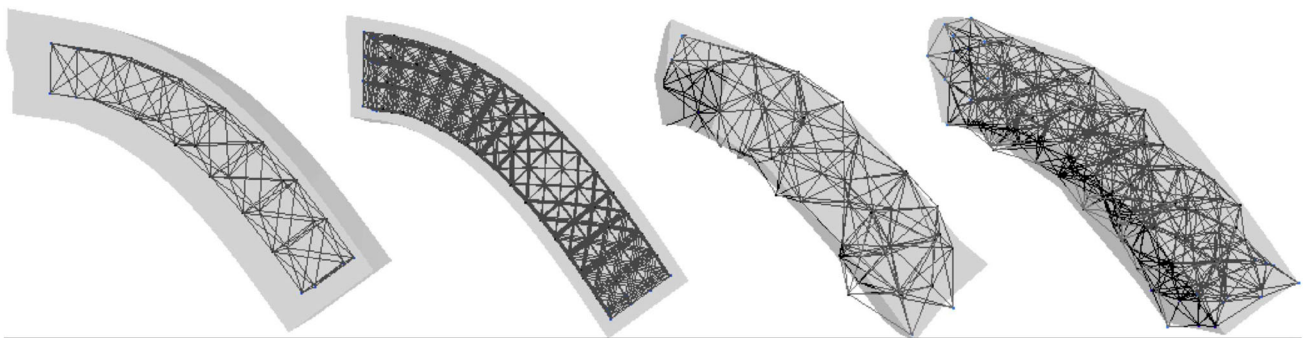
Fig. 14 Deflection test for four different MSMs. In each panel, a wire frame of a MSM model of an elastic bar of dimensions $4a_0 \times 1a_0 \times 1a_0$ is shown together with visual representation of the bar (a mesh within which the MSM is embedded). From the *left* (1) Low resolution cubic MSM, (2) High resolution cubic MSM, (3) Low resolution random MSM, (4) Medium resolution random MSM. Numbers of nodes and springs same as in Fig. 13. Applied force $F = 4.1[k_0a_0]$, Young's modulus $E = 250\,k_0/a_0$

Fig. 15 Cracks forming on a surface of drying material. Top view of a cylindrical block. *Left* cubic lattice MSM, *right* random MSM
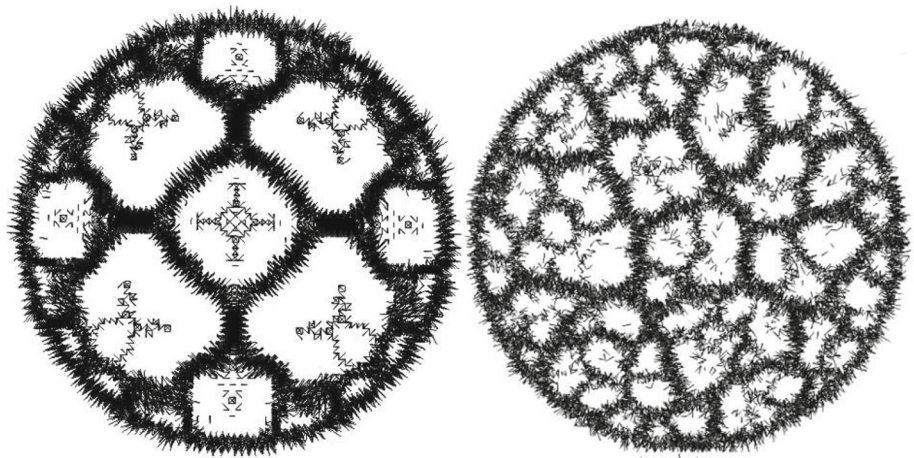
Next, we have measured the elastic properties of both cubic and random lattices in a series of simple test simulations and shown that they agree satisfactory with theoretical predictions and thus are well suited for the modeling of elastic materials. The random MSMs seem to perform almost as good as the cubic ones when the global deformations of the system are concerned, but slightly underperform at the smaller scales (of the order of few internode distances). Even though the difference is not large, it does show that MSMs, particularly low resolution ones, require attention during generation process to minimize discretization errors. Overall, however, the performance of random models is good enough for them to be an attractive alternative to the cubic models, as in many situations a slight decrease of accuracy may be an affordable price to pay for the flexibility of choosing node positions. Disordered MSM may be particularly suitable for simulating fracture or crack propagation. In Fig. 15 we show an example of such application, where it is clearly visible that cracks formed on a lattice-based MSM have a tendency of following specific "propagation" planes inherently defined by the lattice geometry and not the properties of the material. At the same time, disordered MSMs are not influenced by this and the crack patterns are much more natural.

It should also be noted in this context that the random MSM of Fig. 2 is just a simple example of this class of models, given purely for the sake of illustrating the calculation of elastic properties. If desired, a more sophisticated disordered MSMs can be constructed, better tuned to a particular system or purpose in mind; in particular additional attention may be required to properly generate the surface of an object. Importantly, the formalism presented here can also be applied to these more specific systems.

References

1. Baudet, V.; Beuve, M.; Jaillet, F.; Shariat, B.; Zara, F.: Integrating tensile parameters in 3D mass-spring system. Technical Report RR-LIRIS-2007-004, LIRIS UMR 5205 CNRS/INSA de Lyon/Université Claude Bernard Lyon 1/Université Lumiére Lyon 2/École Centrale de Lyon, February (2007)
2. Bower, A.F.: Applied Mechanics of Solids. CRC Press, Taylor & Francis, Boca Raton (2009)
3. Delingette, H.: Triangular springs for modeling nonlinear membranes. IEEE Trans. Vis. Comput. Gr. **14**(2), 329–341 (2008)
4. Hardy, R.J.: Formulas for determining local properties in molecular-dynamics simulations—shock waves. J. Chem. Phys. **76**, 622–628 (1982)
5. Kot, M., Nagahashi, H., Szymczak, P.: Verification of physical properties of materials modeled with mass-spring systems. Technical report of IEICE. Multimed. Virtual Environ. **110**(457), 201–206 (2011)
6. Ladd, A.J.C., Kinney, J.H.: Elastic constants of cellular structures. Phys A Stat. Theor. Phys **240**(1–2), 349–360 (1997)
7. Lakes, R.S.: Deformation mechanisms in negative Poisson's ratio materials: structural aspects. J. Mater. Sci. **26**, 2287–2292 (1991)
8. Landau, L.D., Lifshitz, E.M.: Theory of elasticity. Pergamon, London (1959)
9. Levine JA, Bargteil AW, Corsi C, Tessendorf J, Geist R (2014) A peridynamic perspective on spring-mass fracture. In Proceedings of the ACM SIGGRAPH/Eurographics Symposium on Computer Animation
10. Liu, T., Bargteil, A.W., O'Brien, J.F., Kavan, L.: Fast simulation of mass-spring systems. ACM Trans. Gr. 32(6):209:1–7, Proceedings of ACM SIGGRAPH Asia 2013, Hong Kong. (2013)
11. Lloyd, B.A., Szekely, G.: Harders M (2007) Identification of spring parameters for deformable object simulation. IEEE Trans. Vis. Comput. Gr. **13**(5), 1081–1094 (2007)
12. Love AEH (1906) A treatise on the mathematical theory of elasticity. Cambridge University Press
13. Meier, U., López, O., Monserrat, C., Juan, M.C., Alcañiz, M.: Real-time deformable models for surgery simulation: a survey. Comput. Methods Prog. Biomed. **77**(3), 183–197 (2005)
14. Nealen, A., Müller, M., Keiser, R., Boxerman, E., Carlson, M., Ageia, N.: Physically based deformable models in computer graphics. Comput. Graph. Forum **25**(4), 809–836 (2006)
15. Ostoja-Starzewski, M.: Lattice models in micromechanics. Applied Mechanics Reviews **55**(1), 35–60 (2002)

16. Press, W.H., Teukolsky, S.A., Vetterling, W.T., Flannery, B.P.: Numerical Recipes: The Art of Scientific Computing, 3rd edn. Cambridge University Press, New York (2007)
17. San-Vicente, G., Aguinaga, I., Celigueta, J.T.: Cubical mass-spring model design based on a tensile deformation test and nonlinear material model. IEEE Trans. Vis. Comput. Gr. **18**(2), 228–241 (2012)
18. Torquato, S.: Random Heterogeneous Materials: Microstructure and Macroscopic Properties. Springer, New York (2002)
19. Van Gelder, A.: Approximate simulation of elastic membranes by triangulated spring meshes. J. Graph. Tools **3**(2), 21–42 (1998)
20. Zimmerman, J.A., WebbIII, E.B., Hoyt, J.J., Jones, R.E., Klein, P.A., Bammann, D.J.: Calculation of stress in atomistic simulation. Model. Simul. Mater. Sci. Eng. **12**(4), S319 (2004)

Hiroshi Nagahashi received his B.E. and Ph.D. degree from Tokyo Institute of Technology in 1975 and 1980, respectively. Since 1990, he has been working with Imaging Science and Engineering Laboratory at Tokyo Institute of Technology, where he is currently a professor. His research interests include computer vision, computer graphics, and geometric modeling.

Maciej Kot received his B.E. and M.Sc. degree in Computer Science from Warsaw University of Technology in 2008 and 2010, respectively. He also received an M.Sc. in physics from the University of Warsaw in 2010. Since 2011, he has been studying for a Ph.D. at Tokyo Institute of Technology Imaging Science and Engineering Laboratory. His research interests include computer graphics and physically based modeling and simulation.

Piotr Szymczak received his Ph.D. from the University of Warsaw (Poland) in 2001. After two years of postdoctoral research at the University of Florida he joined the Institute of Theoretical Physics at the University of Warsaw as an assistant professor. His group focuses on the intersection between physics and other fields: from the dissolution of porous or fractured rock to the structure and dynamics of biological soft matter. The approach taken is to model the system in a simple but physically meaningful way, and then explore the model using the combination of analytical and numerical techniques.